International Journal of Nanomedicine

Dovepress
open access to scientific and medical research

Open Access Full Text Article

ORIGINAL RESEARCH

Hyaluronic Acid Micelles for Promoting the Skin Permeation and Deposition of Curcumin

Jiangxiu Niu*, Ming Yuan*, Zhaowei Zhang, Liye Wang, Yanli Fan, Xianghui Liu, Xianming Liu, Huiyuan Ya, Yansong Zhang, Yang Xu

College of Food and Drug, Henan Functional Cosmetics Engineering & Technology Research Center, Luoyang Normal University, Luoyang, 471934, People's Republic of China

*These authors contributed equally to this work

Correspondence: Liye Wang; Xianming Liu, Email liye2009314@163.com; myclxm@163.com

Background: The poor skin permeation and deposition of topical therapeutic drugs is a major issue in topical drug delivery, improving this issue is conducive to improving the topical therapeutic effect of drugs.

Methods: In this study, octadecylamine modified hyaluronic acid (OHA) copolymer was synthesized by amide reaction technique to prepare curcumin (CUR)-loaded micelles (CUR-M) for topical transdermal administration. CUR-M was successfully prepared by dialysis, and the formulation was evaluated for particle size, zeta potential, surface morphology, entrapment effciency (EE%), drug loading (DL), X-ray diffraction (XRD), Fourier transform infrared spectroscopy (FTIR) and the in vitro drug release. Additionally, in vitro skin permeation and retention, in vivo topical analgesic and anti-inflammatory activity, and skin irritation were assessed.

Results: The mean drug loading (DL), drug entrapment efficiency (EE), hydrodynamic diameter and zeta potential of CUR-M were 8.26%, 90.86%, 165.64 nm and −26.85 mV, respectively. CUR-M was characterized by X-ray diffraction (XRD) and Fourier transform infrared spectroscopy (FTIR), it was found that there was an interaction between CUR and OHA, and CUR existed in CUR-M in an amorphous form. CUR-M exhibited sustained release in 48 h and good stability at 4 °C for 21days. CUR-M could significantly increase the skin penetration and retention of CUR and had better analgesic and anti-inflammatory activities in vivo when compared with CUR solution. Hematoxylin-eosin staining results revealed that the transdermal penetration mechanism of CUR-M might be related to the hydration of stratum corneum by HA. In addition, CUR-M showed no skin irritation to mouse skin.

Conclusion: CUR-M might be a promising and safe drug delivery system for the treatment of topical diseases.

Keywords: topical drug delivery, hyaluronic acid, micelles, curcumin, skin permeation and deposition

Introduction

As an important route of drug administration, transdermal delivery for topical therapy has many advantages, such as targeting the treatment site, reducing the risk of systemic side effects, improving patient compliance and medication flexibility, etc.[1] For topical formulations, the goal of formulation design is to maximize drug penetration through the stratum corneum and retention in the skin to increase the skin bioavailability of the drug.[2] However, the skin barrier function restricts most drugs from entering and accumulating in the skin to achieve effective therapeutic concentrations, resulting in drug waste and suboptimal clinical efficacy after topical administration.[3] The most important function of the skin is to prevent chemicals, microorganisms and other harmful substances from invading the human body, so as to ensure that the human body is not infringed in a relatively hostile environment. It is well known that the physical barrier function of the skin mainly results from the stratum corneum, the outermost layer of the skin. Stratum corneum is a firm, flat, dry and keratinized brick wall composed of horny dead cells. In addition, the cell membrane of stratum corneum is thick and the cell matrix is rich in flexible proteins and lipids.[3] These structural features determine that the stratum corneum becomes the main barrier for drug percutaneous penetration.[4]

Received: 28 April 2022
Accepted: 29 August 2022
Published: 7 September 2022

Overcoming the stratum corneum barrier and improving the topical bioavailability of drugs is not only the main problem of topical drug delivery but also the challenge of effective topical administration.[5] Various nano-drug delivery systems have been developed to overcome the problems of topical drug administration, and nano-carriers that have gained importance so far include micelles, ethosomes, solid lipid nanoparticles, nanoemulsions, etc.[6] Nano-scale polymeric micelles are colloidal carriers with a core–shell structure formed by self–aggregation of amphiphilic polymers in aqueous media when the concentration of polymers is higher than the critical micelle concentration. Therefore, the polymer micelle formulation will improve the solubility and stability of insoluble drugs by encapsulating the drugs in the micelle core and away from the aqueous solution. The micelles could enter the skin through pathways of intercellular, transcellular and skin appendages, and their skin permeation and retention capacities depend on the type of micellar material, the size and zeta potential of the micelles.[7,8] Once the micelles enter the skin through the stratum corneum, they are likely to sustained release the drug into the skin tissue. In addition, studies had shown that copolymer micelles could enhance the penetration and retention of drugs in the skin and reduce drug absorption into the systemic circulation.[5] Therefore, the development of polymeric micelle formulations is considered as one of the suitable carriers that can selectively act on the topical skin.

Hyaluronic acid (HA) is a biomaterial composed of N-acetyl-D-glucosamine and glucuronic acid, widely distributed in the extracellular matrix (ECM) of connective tissue, and has a variety of important biological functions, such as cell signaling, wound healing, joint lubrication, skin moisturizing, etc.[9] There is a large amount of HA in human skin, accounting for more than 50% of the total hyaluronic acid in the body. In addition, hyaluronic acid can penetrate and remain in the skin through hydration, bioadhesion, hydrophobic interactions and viscoelasticity.[10] In general, low molecular weight HA has a higher skin penetration capacity than larger weight HA. HA can be prepared into suitable drug carriers by chemical modification while maintaining its biological function and biodegradability.[11] In recent years, HA-based self-assembled formulations have been investigated in transdermal delivery. For instance, HA–Cholesterol self-assembled nanoparticles and hydrotropic nicotinamide were developed to enhance the permeation of tacrolimus (FK506) in the treatment of psoriasis.[12] HA–dodecylamine-based nanohydrogels was developed to deliver and penetrate indocyanine green (ICG) deep into the skin for the treatment of neurological disorders.[13] In addition, various forms of HA-based drug delivery systems including transfersomes, niosomes, hydrogels and microneedle patches have also been developed to enhance drug permeation through and into the intact skin or inflamed skin for topical disease treatment.[14–17]

Curcumin (CUR) is a polyphenolic compound isolated from the turmeric plant. CUR has various pharmacological activities, such as analgesic, anti-inflammatory, anti-viral, anti-tumor and anti-oxidant. However, its poor water solubility and susceptibility to intestinal and hepatic metabolism limit its application via the oral route.[18] Hence, the route of topical transdermal administration might be a potential alternative for the delivery of CUR into local treatment site. Various drug delivery carriers, such as nanovesicles, nanoemulsions and ethosomes, had been used to improve the effectiveness of transdermal administration of CUR.[1,19]

Herein, we present the design and synthesis of octadecylamine modified hyaluronic acid (OHA) copolymer. The copolymer was used in the preparation of CUR-loaded micelles (CUR-M) to achieve the topical transdermal delivery of CUR (Figure 1). The chemical structure of OHA copolymer was confirmed by ^{1}H NMR, and its critical micelle concentration (CMC) was determined by fluorescence probe method. The pharmaceutical properties of CUR-M were investigated via particle size, zeta potential, surface morphology, powdered X-ray diffraction (PXRD), Fourier transform infrared spectroscopy (FTIR), in vitro release and stability. The in vitro skin permeation and retention, transdermal penetration mechanism, intradermal drug distribution, in vivo analgesic and anti-inflammatory activities and in vivo skin irritation CUR-M for topical delivery were also investigated.

Materials and Methods

Materials

Hyaluronic acid (MW < 10 *k*Da) was obtained from Freda Biochem Co., Ltd. (Shandong, China). Octadecylamine was purchased from Aladdin (Shanghai, China). (3-dimethylaminopropyl)-3-ethylcarbodiimide hydrochloride (EDC.HCL) and N-hydroxysuccinimide (NHS) were purchased from Nanjing dulai Biotechnology Co., Ltd (Nanjing, China).

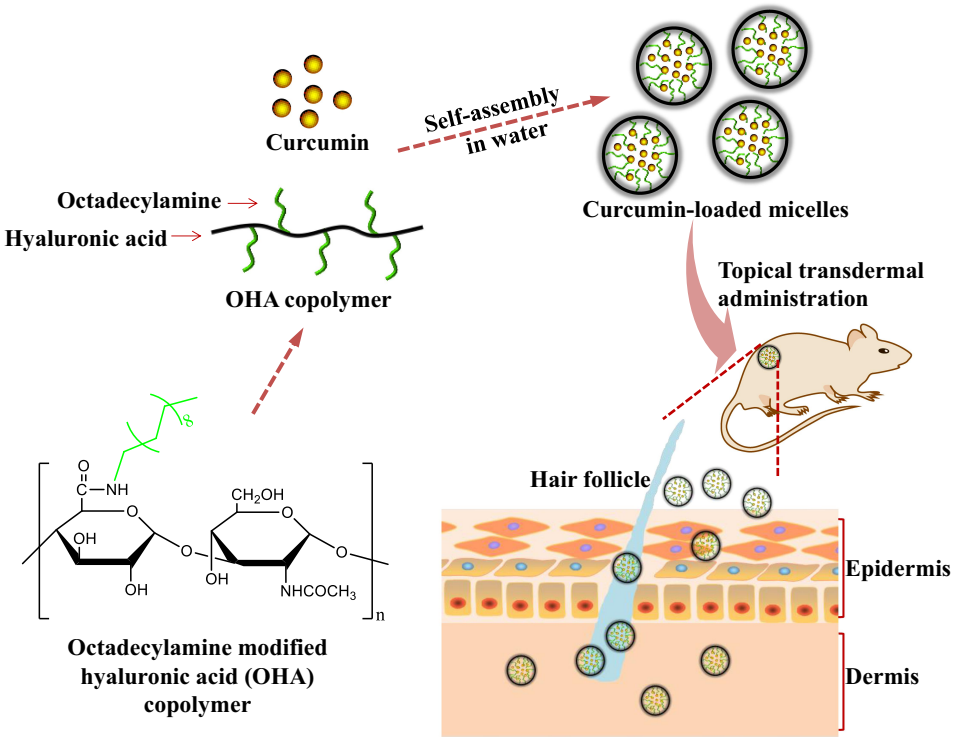

Figure 1 Schematic illustration of the CUR-loaded micelles (CUR-M) based on OHA copolymer for promoting the skin permeation and deposition of CUR.

Curcumin was purchased from Xi'an Ivy Biotechnology Co. Ltd (Xian, China). All other reagents were analytical grade preparation.

Animals

ICR mice weighing 18−22 g and Sprague-Dawley rats weighing 200−220 g were obtained from the Henan Experimental Animal Center, Zhengzhou, China. All animals were housed in a constant temperature and humidity room with a 12 h light cycle and had free access to food and tap water before the experiments. The experimental protocols were in accordance with the guidelines approved by Luoyang Normal University, and all procedures were performed after approval from Institutional Animal Ethics Committee.

Synthesis and Characterizations of OHA

Octadecylamine modified hyaluronic acid (OHA) copolymer was synthesized by covalently linking the carboxyl group of HA and the amino group of octadecylamine via an amidation reaction according to the literature with minor modifications.[20,21] In brief, 100 mg of HA was dissolved in 10 mL of deionized water by naturally swell. When the HA was fully dissolved, 100 mg of EDC and 60 mg of NHS were added and stirred at room temperature for 6 h to activate the carboxyl group of HA. About 71.1 mg of octadecylamine was then dissolved in 5 mL of dimethylformamide (DMF) and slowly added to the activated HA solution. The mixed solution was stirred at 60 °C to react for 5 h. Subsequently, the mixture was stirred for a further 24 h at room temperature. The ultimate reaction solution was transferred to a dialysis bag (MWCO = 3500) and then dialyzed against ethanol/deionized water (V/V, 7:3, 5:5, 3:7) for 48 h, followed by dialysis against deionized water for 48 h to remove organic solvents and soluble side products. Finally, the solution was filtered with 0.45 μm microporous membrane to remove other impurities. The filtrate was lyophilized for 24 h to obtain OHA copolymer. The structure of the OHA was characterized by ^{1}H NMR using an apparatus (AVANCE500, Bruker, Germany) at 25 °C.

The critical micelle concentration (CMC) of OHA copolymer was determined by fluorescence probe method.[22] Briefly, 0.1 mL of pyrene solution (6.0×10^{-6} mol/L) was added in a brown glass vial and placed in the dark for 24 h to

evaporate off the acetone. Then, OHA aqueous solutions, ranging from 0.0005 to 0.5 mg/mL were added to reach a final pyrene concentration of 6.0×10^{-7} mol/L, and the resulting samples were subjected to water bath ultrasound for 30 min. The mixture solution was incubated in a darkroom for 12 h. The emission spectrum of fluorescent pyrene was recorded using a fluorescence spectrophotometer (F-7000; Hitachi, Tokyo, Japan) at an excitation wavelength of 335 nm. The fluorescence emission spectra of pyrene were collected at a wavelength range of 350−550 nm with an emission bandpass of 5 nm.

Preparation and Characteristics of CUR-M

OHA (80 mg) and CUR (8 mg) were dissolved in 5mL DMSO and then dialyzed (dialysis bag, MWCO 3.5 kDa) in dark for 24 h. The resulting mixture was filtered with a 0.22 μm microporous membrane to remove un-encapsulated drug and other impurities. Blank micelles without any drug were prepared by the same preparation process.

The CUR content in CUR-M was determined by UV–Vis spectrometry at 425 nm (TU-1810PC, Purkinje, Beijing, China). The drug loading (DL) and entrapment efficiency (EE) of CUR-M were calculated according to the following equations:

$$\mathrm{DL}\% = \frac{\text{Weight of the drug loaded in micelles}}{\text{Weight of the feeding polymers and drug}} \times 100\%$$

$$\mathrm{EE}\% = \frac{\text{Weight of the drug encapsulated in micelles}}{\text{Weight of the feeding drug}} \times 100\%$$

The particle size distribution of CUR-M were analyzed by dynamic light scattering (DLS) using a Zetasizer ZS90 (Malvern Instruments, UK) at a constant temperature of 25 °C with the scattering angle of 90 degrees after equilibration for 120 s, and zeta potential was determined simultaneously. Samples were diluted 10-fold with deionized water before determination.

The surface morphology of CUR-M was observed by scanning electron microscope (SEM) (Sigma 500, ZEISS, Germany). The 30-fold diluted CUR-M dispersion was dropped on a silicon substrate and air-dried overnight. The samples were then coated with gold using a sputter coater under vacuum before observation. The same method was used to observe the surface morphology of lyophilized CUR-M powder.

X-Ray Diffraction (XRD) and Fourier Transform Infrared Spectroscopy (FTIR)

XRD measurement of CUR, physical mixtures of CUR and OHA, lyophilized blank micelles and CUR-M were performed using an X-ray powder diffractometer (D8 ADVANCE, Bruker, Germany) with Cu Kα radiation. The operating voltage and current were set at 40 kV and 40 mA, respectively, and the scattering angle 2θ was set in the range of 5°−70°.

FTIR spectra were obtained using a Nicolet 6700 Fourier transform infrared spectrophotometer (Thermo Fisher Scientific, USA). Using the KBr tableting method, appropriate samples of CUR, physical mixtures of CUR and OHA, lyophilized blank micelles and CUR-M were, respectively, mixed uniformly with KBr as the samples, and then pressed into thin pellets. These pellets were scanned in the wavenumber range of 4000−400 cm^{-1}.

In vitro Release Studies

The in vitro release of CUR from tested formulation was performed in phosphate buffer solution (PBS, pH 7.4) containing ethanol (40%, v/v) using a dialysis method (MWCO, 3.5k Da). CUR solution (equivalent to 1.0 mg of CUR) was used as a control, dialysis bags containing 2.0 mL of CUR-M were sealed and immersed into 20 mL of release medium. The release medium was kept at 37 °C and stirred at 300 rpm with a magnetic stirrer. At predetermined time points, 1.0 mL of release medium was withdrawn. Subsequently, an equal volume of fresh release medium pre-warmed to 37 °C was added immediately to maintain sink conditions. The content of CUR was measured using a fluorescence spectrophotometer set with Ex = 442 nm and Em = 475 nm (F-7000, Hitachi High-Technologies Corporation, Japan).

Stability of CUR-M

To evaluate the stability of CUR-M, the content of CUR in micelles was determined after storage for 0, 7, 14 and 21 days, the EE and DL were calculated. All samples were stored at 4°C in the dark.

In vitro Skin Permeation and Retention Studies

The rats were sacrificed by excessive inhalation of diethyl ether. After the abdominal hair of the rats was shaved with an electric razor, the abdominal skin was separated, and the adhered fat and other subcutaneous tissue were carefully excised. The prepared full-thickness skin was then rinsed with physiological saline solution and stored in a refrigerator at −20 °C with the restriction of usage within one week. Prior to usage, the skin was thawed by exposure to physiological saline solution for 15 min and the integrity of the skin was examined.

In vitro skin permeation and retention studies were performed by using a vertical glass Franz diffusion instrument (RYJ-6B, Shanghai Huanghai Drug Control Instrument Co., Ltd, China). The skin was clamped between the donor and the receptor compartment of the Franz diffusion cell, with the epidermal side facing the donor compartment and the dermis side in contact with the diffusion medium. The effective penetration area was 2.8 cm^2, and the receptor compartment capacity was 6.8 mL. The receptor compartment was filled with diffusion medium (pH 7.4 phosphate buffer with 40% of ethanol). The temperature of the diffusion cells was maintained at 37 ± 0.5 °C using a recirculating water bath, and the diffusion medium in the receptor compartment was constantly stirred with a magnetic bar at 300 rpm. The formulations, CUR and CUR-M, were gently placed in the donor side, respectively, with an amount equivalent to 0.15 mg of CUR. At 2, 4, 6, 8, 10, 12 and 24 h, 1.0 mL of diffusion medium in the receptor compartment was collected and replenished immediately with an equal amount of diffusion medium to maintain sink conditions. Then, the samples were quantified using a high-performance liquid chromatography (HPLC) system (U-3000, Thermo, USA) with a UV detector and a Wondasil C18 column (5 mm, 200 × 4.6 mm). The mobile phase consisted of acetonitrile, 0.5% phosphoric acid at a ratio of 58:42 (v/v). The UV visible detector and operating temperature was set to 423 nm and 30 °C, respectively. The flow rate was 1.0 mL/min, and injection volume was 20 μL. The cumulative amount of CUR permeated through rat skin per unit area was calculated, and the permeation profile was plotted as a function of time.

In order to determine the amount of CUR retained in the skin, the skin was carefully separated from the diffusion cell at the end of skin permeation experiments (24 h) and rinsed with deionized water to remove any residual formulation, and then the skin was finely sheared into small pieces and soaked in 2 mL of methanol for 24 h with constant stirring in the dark. The retained CUR in skin samples was extracted by four ultrasonic cycles of 30 min in KQ-100 untrasound bath (Kunshan, China), followed by centrifugation at 12,000 rpm for 15 min to separate the supernatant. The supernatant was then filtered by a membrane (0.22 μm), and the content of CUR was analyzed by HPLC. The amount of CUR retained in skin was calculated.

Hematoxylin–Eosin Staining

The hair on the back of the mice was carefully shaved with an electric shaver 24 h before the experiment. Subsequently, cotton pieces (1 cm^2) were impregnated with 0.2 mL of normal saline, CUR solution and CUR-M, respectively, and then placed on the back of the mice and fixed with medical tape. After 6 h, the animals were humanely sacrificed, and the regions of the skin that received the topical treatment were carefully excised. The residual samples were removed with physiological saline. The skin samples were then fixed with 4% paraformaldehyde, dehydrated with ethanol and made transparent with dimethyl benzene to prepare paraffin sections for hematoxylin-eosin staining. Photographs of paraffin sections were acquired using CaseViewer 2.3 (3DHISTECH Ltd, Hungary) at room temperature.

Confocal Laser Scanning Microscopy (CLSM) Study

The mice skins were treated with CUR solution and CUR-M according to the same procedure as in the hematoxylin–eosin staining experiments (Hematoxylin–Eosin Staining). The drug administration lasted for 1 h and 6 h, and then the skin was excised and washed with physiological saline. Slice samples of the skin longitudinal section were prepared via a freezing slicer (Leica CM 1950, Germany). The skin sections were nucleus counterstained with DAPI, and the skin

permeation of the formulation was observed by using a confocal laser scanning microscope (CLSM, LEICA TCS SP5, Leica, Germany) with EX/Em wavelength of 425/515 nm.

In vivo Hot Plate Test in Mice

The analgesic activity in mice was investigated using the hot plate method to evaluate the effect of the developed drug-loaded micelles on the transdermal administration of CUR.[23] Briefly, female ICR mice weighing 18–22 g (n = 10 per group) were placed on a hot plate apparatus (YLS-6B, Jinan, China). The hot plate temperature was controlled at 55 ± 0.5 °C and surrounded by a transparent cylinder to confine the mice to the hot plate during the test. Only mice with a baseline latency of 10–30 seconds were used in the study. Mice were topical transdermal administered CUR solution or CUR-M at 15 mg/kg, physiological saline was used as the control group. The latency was the reaction time recorded when mice first licked their hind paw or jumped from the surface of the hot plate after being placed on the hot plate. If these behaviors were not observed within 60s, the animal was removed from the hot plate to protect the paw from damage. The post-drug latency was measured at 30, 60 and 120 min after topical transdermal drug administration.

Dimethyl Benzene Induced Mice Ear Edema Test

The anti-inflammatory activity of the developed formulation was studied using the dimethyl benzene induced acute ear edema test. Thirty mice were randomly divided into three groups (n = 10 per group). The right ear of mice in groups I, II and III was administered with 0.1 mL of the tested formulation with a drug concentration of 0.08% (w/v), respectively. After 1 h administration, dimethyl benzene (30 μL per mouse) was dropped on both sides (15 μL per side) of the right ear. The left ear was not treated with formulation and dimethyl benzene to serve as a control. The mice were humanely sacrificed after treatment with dimethyl benzene for 30 min, and then the same area of the left and right ears of the mice was cut off with an 8 mm punch. After precise weighing, the values of ear edema were obtained by calculating the weight difference between the left and right ear pieces, and the inhibitory ratios of ear edema were calculated according to the values of ear edema.

Skin Irritation Studies

The skin irritation of the developed formulation was investigated in female mice to evaluate the safety of the formulation.[24,25] Twenty-four hours before the experiment, the hair on both sides of the spine (approximately 3 cm^2) was carefully removed with an electric razor without causing epidermal damage, and the mice were divided into three groups with six mice in each group. First group of mice received physiological saline and served as control, while second and third groups of mice received CUR solution and CUR-M, respectively. The filter paper (2 cm^2) was impregnated with 0.3 mL of different formulations, pasted on the back of the mouse and then fixed with medical tape. The residual formulation was removed by scrubbing with warm water after 4 h application of various formulations. The skin was observed for visible skin irritation properties such as irritation and edema at 1, 4, 24, 48 and 72 h after removing the residual formulation.

Statistical Analysis

All data were expressed as mean values ± standard deviations (mean ± SD) from at least three independent experiments. The results were analyzed by using Student's *t*-test and statistical differences between two groups were evaluated and considered significant for $p < 0.05$.

Results and Discussion

Synthesis and Characterizations of OHA

In this paper, amphiphilic polymer of OHA was synthesized by amide reaction between −COOH groups of HA molecule and $-NH_2$ groups of octadecylamine molecule in the presence of EDC and NHS. The synthetic scheme for OHA is shown in Figure 2A. The ^{1}H NMR spectra (Figure 2B) were used to identify the chemical structure of OHA. The characteristic peaks of OHA are shown in Figure 2B. In the ^{1}H NMR spectrum of OHA, peaks at about 0.97 ppm were

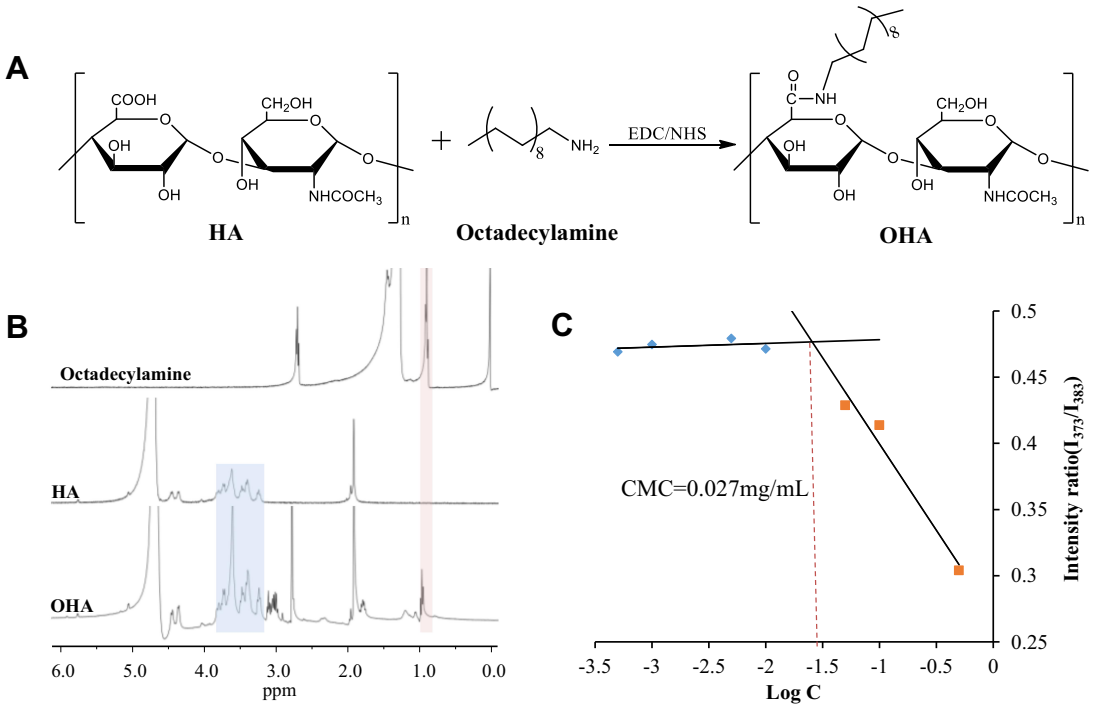

Figure 2 Synthesis and characterizations of OHA. (**A**) Synthetic scheme for OHA. (**B**) ^{1}H NMR spectras of HA, octadecylamine and OHA. (**C**) The intensity ratio (I_{373}/I_{383}) of pyrene fluorescence as a function of OHA concentration.

attributed to protons of the –CH_3– group of octadecylamine, peaks ranging from 2.99 to 4.05 ppm were attributed to protons of the glycosides in HA and peaks at about 2.32 ppm were attributed to protons of the newly groups of –NHCO–. The results confirmed that OHA was successfully constructed. The degree of substitution (DS) of octadecylamine was 15.4 ± 0.25%, which was calculated from the integral ratio of the peak at δ 0.97ppm to the peak at δ 1.91ppm in the ^{1}H NMR spectrum of OHA.

OHA is an amphiphilic polymer, so it can self-assemble to form polymeric micelles in the aqueous phase. The critical micelle concentration (CMC) of OHA in water was determined using pyrene as a fluorescent probe. It is generally believed that hydrophobic pyrene molecules have low solubility and spectral intensity in the aqueous phase. However, when there is a certain concentration of amphiphilic molecules in the aqueous environment, pyrene molecules could be encapsulated and exist in the hydrophobic core of amphiphilic molecules, and their solubility and fluorescence intensity will increase greatly. The CMC of amphiphilic polymer could be calculated by comparing the changes of I_{373}/I_{383} ratio of pyrene molecules under different conditions. The CMC of OHA was 0.027 mg/mL (Figure 2C), which was much lower than that of the low-molecular-weight surfactant.[26] CMC is an important factor in the use of amphiphilic polymers in drug delivery systems. In general, lower CMC could avoid the disintegration of micelles caused by the dilution of body fluid, which is beneficial to the stability of micelles under highly diluted conditions.[27]

Characterization of CUR-M

OHA was used to prepare CUR-M via a dialysis method. The DL and EE drug-loaded micelles were found to be 8.26 ± 0.16% and 90.86 ± 1.12%, indicating that most CUR was entrapped in the hydrophobic core of the micelles. Research report showed that the solubility of curcumin in water was 0.39 μg/mL.[28] After being encapsulated in OHA, the water solubility was increased to 1.47 mg/mL, 3.77 × 10^3 times higher than that of crude CUR.

The particle size of blank micelles measured by DLS was 149.51 ± 2.16 nm. After loading CUR, Cur-M presented a slightly increased particle size of 165.64 ± 0.22 nm. The slightly increased particle size of the CUR-M might be due to the fact that the CUR encapsulated in the hydrophobic core of micelles. The particle size distribution of CUR-M

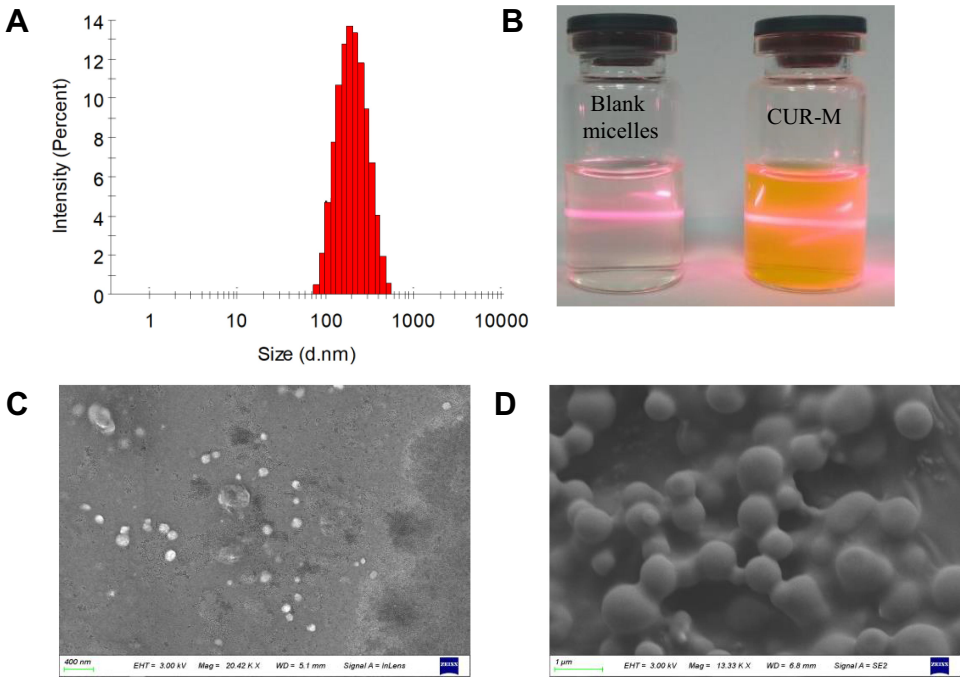

Figure 3 Characterization of CUR-M. (**A**) Particle size distribution of CUR-M. (**B**) Appearance and Tyndall characterization. (**C**) SEM image of CUR-M dispersion. (**D**) SEM image of lyophilized CUR-M powder.

was homogeneous (Figure 3A). The small particle size of drug loaded micelles is important, because it is beneficial to increase the contact area of micelles with skin tissue and influence the interaction of micelle particles with skin tissue. Furthermore, studies had shown that smaller particles are considered to penetrate deep into the skin appendages, thereby increasing the penetration and deposition of drug-loaded particles in the skin tissue.[2] The zeta potential was measured as −26.85 ± 0.67 mV. The negative charge on the surface of micelles is conducive to the physical stability of drug loaded micelles in aqueous solution. The prepared CUR-M formed a yellow transparent liquid, with laser-induced Tyndall phenomenon (Figure 3B), which is an essential feature of colloidal liquid. By SEM, both CUR-M dispersion and lyophilized CUR-M powder appeared to be spherical structure with a relatively uniform size (Figure 3C and D).

XRD and FTIR Study

Figure 4A presents the XRD results for CUR powder, physical mixtures of CUR and OHA, lyophilized blank micelles and CUR-M. CUR exhibited sharp diffraction peaks at 2θ = 8.72°, 17.18°, 19.38°, 25.48°, suggesting that it had a crystalline structure.[29] The XRD pattern of lyophilized blank micelles and CUR-M showed that they did not present the sharp diffraction peaks of CUR but exhibited a broad peak in the range of 16°−27°, confirming their amorphous characteristics. It indicated that a large number of amorphous substances were formed during the preparation of CUR loaded micelles. The disappearance of the crystallization peaks of CUR provided evidence for the formation of micelles.

Figure 4B shows the FTIR spectra of CUR powder, physical mixtures of CUR and OHA, lyophilized blank micelles and CUR-M. The principal peaks of CUR were observed at 3509.36 cm^{-1} and 1629.37 cm^{-1}, which correspond to the –OH stretch and –C=O stretching, respectively. In addition, band at 962.48 cm^{-1} owing to the –CH stretching band of alkene chain present in CUR was also observed.[30] For blank micelles, the band at 1048.92 cm^{-1} could be due to the C–O–C stretching vibration of HA.[31] After encapsulation of CUR in micelles, the characteristic peaks of CUR at 3509.36 cm^{-1}, 1629.37 cm^{-1} and 962.48 cm^{-1} were disappeared. This change indicated that there might be hydrogen bond interactions among the groups of CUR and the OHA. These interactions assisted in the encapsulation of CUR into copolymer micelles and facilitated the slow and sustained release of CUR from CUR-M dispersions.

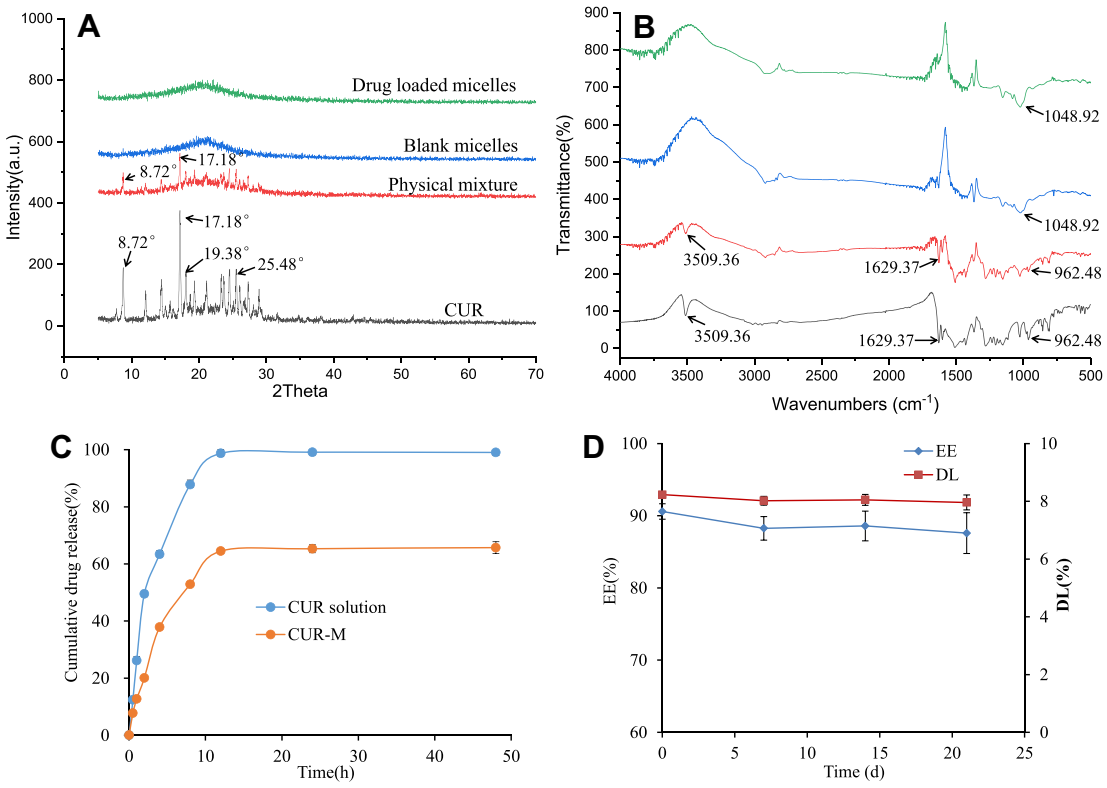

Figure 4 (A) X-ray diffraction patterns and (**B**) FTIR of CUR, physical mixtures of CUR and OHA, lyophilized blank micelles and CUR-M. (**C**) The in vitro release of CUR from CUR-M and CUR solution in PBS of pH 7.4 (n=3). (**D**) stability of CUR-M.

In vitro Release Studies

Figure 4C shows the in vitro release behavior of CUR-M and CUR solution in pH 7.4 PBS. The release of CUR from CUR solution was fast, which released almost completely at 12 h. Compared with CUR solution, CUR-M exhibited slow, controlled and sustained release in pH 7.4 PBS, indicating that most of the drug was encapsulated in the hydrophobic core of the micelles.[32] At 48 h, the cumulative release of CUR-M and CUR solution in pH 7.4 PBS were 65.72% and 99.06%, respectively. The slow and sustained release of CUR-M might be due to the hydrogen bond interactions among the groups of CUR and the OHA (discussed in XRD and FTIR Study). Thus, instead of the quick release mode of the CUR solution, the sustained release of CUR-loaded micelles could be used as a CUR reservoir to maintain the sustained release of CUR when exerting local efficacy, so as to prolong the action time of drugs.

Stability Study

The EE and EL of CUR-M were measured at each time point to investigate its stability at 4 °C. From the results shown in Figure 4D, it could be seen that the mean EE was between 87.44% and 90.59% and the DL was between 7.96% and 8.23%, with negligible changes throughout the storage period. This result indicated that the CUR-M had good stability.

In vitro Skin Permeation and Retention Studies

The main purpose of the present study was to promote the skin permeation and deposition of CUR. In vitro drug penetration and retention studies were performed for CUR solution and CUR-M through rat abdominal skin. Figure 5A shows the cumulative amount of CUR permeated across excised rat skin as a function of time. The cumulative amount of CUR permeated through the skin at the end of 24 h was 5.21 ± 0.99 μg/cm^2 for the CUR-M, while it was 1.07 ± 0.18 μg/cm^2 for the CUR solution. The cumulative amount of drug that permeated the skin was significantly higher for CUR-M compared to the CUR solution ($p < 0.01$). The strong water absorption capacity of HA might cause the strong hydration of the stratum corneum layer, resulting in swelling of keratinocytes, rupture of keratinocytes, and changes in the microstructure of the

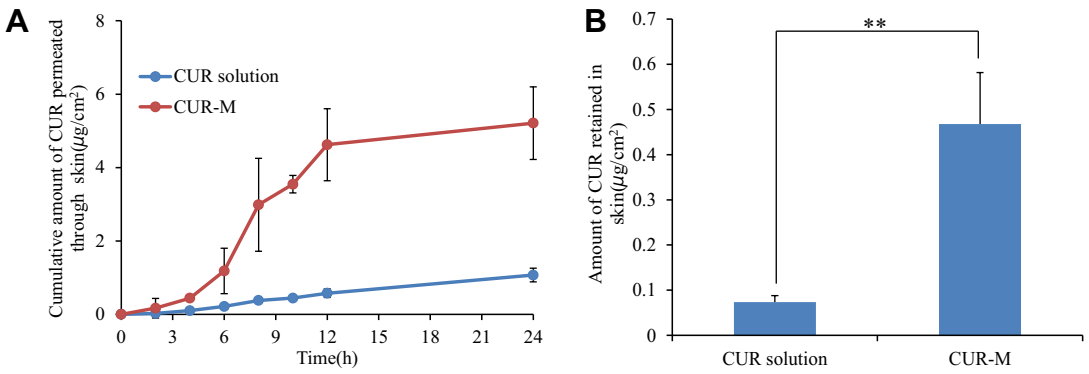

Figure 5 (**A**) In vitro skin permeation profiles of CUR from CUR solution and CUR-M. (**B**) CUR retention in rat skin after exposure to CUR solution and CUR-M for 24 h. Results were presented as mean ± SD (n=3; $^{**}p < 0.01$).

phospholipid bilayer of cells.[33] Therefore, the hydration of skin by HA might contribute to the enhanced transdermal permeability observed for the formulated CUR. The therapeutic efficiency of topically applied drugs depends on the drug concentration in the skin tissue, which is related to the skin penetration ability of the drug in the formulation. The ability of CUR-M to penetrate the skin is stronger than that of the CUR solution, indicating that higher drug concentrations could be obtained in the skin, which is ideal for effective treatment of topical diseases.[34,35]

The drug retention study showed that, after 24 h, the amount of CUR retained in the skin for the CUR-M was 0.47 ± 0.11 μg/cm^2, while the CUR solution was only 0.07 ± 0.01 μg/cm^2 (Figure 5B). The CUR-M achieved good skin retention of CUR, 6.7-fold higher than that of CUR solution. Thus, the amount of drug retained in the skin for the CUR-M was found to be significantly higher ($p < 0.01$) than that of the CUR solution. The increased skin retention of CUR-M for topical delivery could be explained as follows: Firstly, bioadhesive property of HA resulted by the interaction of the hydrophobic domain of HA carbon chain with stratum corneum and the strong affinity of hyaluronic acid to keratin,[36,37] leading to higher skin deposition of CUR-M. Secondly, the large molecular weight of HA might be trapped in skin tissue with limited mobility,[10] which eventually increased the retention of the formulation. Thirdly, the follicular pathway plays an important role in the transdermal delivery pathway and reservoir of topically applied drugs, where nano-sized particles could accumulate in the hair follicle and act as a drug reservoir to prolong drug diffusion into surrounding cells.[38] This might be beneficial to skin deposition of CUR-M. Hence, we could state that the enhanced CUR retention in the skin is mainly attributed to the property of HA and the nano-sized particles of CUR-M.

Hematoxylin–Eosin Staining

To study the transdermal penetration mechanism of CUR-M, the effect of topical administration on skin microstructure in mice by Hematoxylin–eosin staining was observed. Micrographs of hematoxylin-eosin stained mice skin sections after the mice were treated with physiological saline, CUR solution and CUR-M are shown in Figure 6. Hematoxylin-eosin staining showed that the mice skin was composed of epidermis and dermis. In the physiological saline group and CUR solution group, the skin structure of the normal saline was complete, the layers of the epidermis were dense and neat, the layers were clearly visible, the connection was tight, and less keratin fragments could be observed. After treatment with

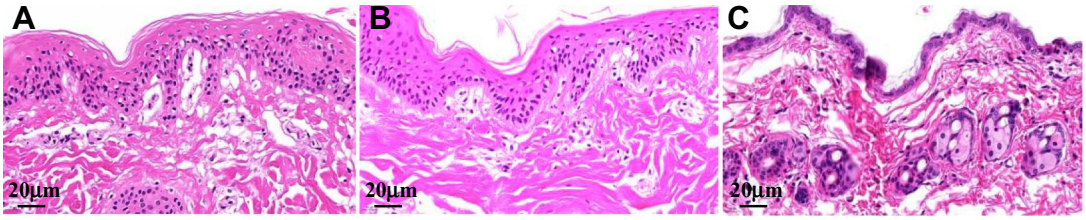

Figure 6 Micrographs of hematoxylin-eosin stained mice skin sections after the mice were treated with physiological saline (**A**), CUR solution (**B**) and CUR-M(**C**).

CUR-M, the stratum corneum was loose and thin, the keratin fragments and intercellular space of the spinous layer increased, the basal layer cells were loosely arranged, which indicated that the promoting skin permeability of CUR-M was related to its change of skin epidermal microstructure. This might be due to the fact that HA was a highly absorbent molecule that could hydrate the stratum corneum, causing swelling and rupture of keratinocytes, leading to changes in the microstructure of the stratum corneum, and ultimately facilitating drug penetration by weakening the barrier effect of the stratum corneum.[39,40] This destruction of the stratum corneum by HA was reversible; once HA was removed, the skin barrier could be easily restored.[36]

Fluorescence Microscopy Imaging

In vivo skin penetration study was performed to investigate the effect of CUR-M on the skin permeation, retention and intradermal drug distribution using confocal laser scanning microscopy (CLSM) images. The CLSM images of the longitudinal sections of the skin of living mice of CUR solution and CUR-M are shown in Figure 7. It could be seen that after 1 h permeation of formulation, only weak fluorescence was observed in the skin and hair follicles for the CUR solution. In contrast, the CUR-M was observed with enhanced fluorescence in both the skin stratum corneum and hair follicles. According to literature reports, the follicular route is the preferred permeation pathway for amphiphilic polymeric micelles.[41] Therefore, for CUR-M, its compact structure, nanoscale hydrodynamic radius and good diffusivity could make it easy to penetrate and retain through the follicular pathway.[42,43] The intradermal fluorescence intensity increased with the increase of penetration time. After 6 h of permeation, CUR solution group showed only slightly enhanced fluorescence in skin and hair follicles, while CUR-M group appeared many strong fluorescent spots in skin and hair follicle. So, like in vitro skin penetration and retention experiments, fluorescence microscopy results also showed that micelles significantly promoted drug penetration and retention in the skin when compared with CUR solution.

Assessment of Analgesic Activity

In this study, we investigated the effect of the developed formulation of CUR-M on the analgesic bioactivity using the standard mice hot plate test, which is a fully validated experimental method for evaluating analgesic agents. The principle of the method is based on the test of two behavioral reactions of hind paw licking and jumping. Figure 8A shows the

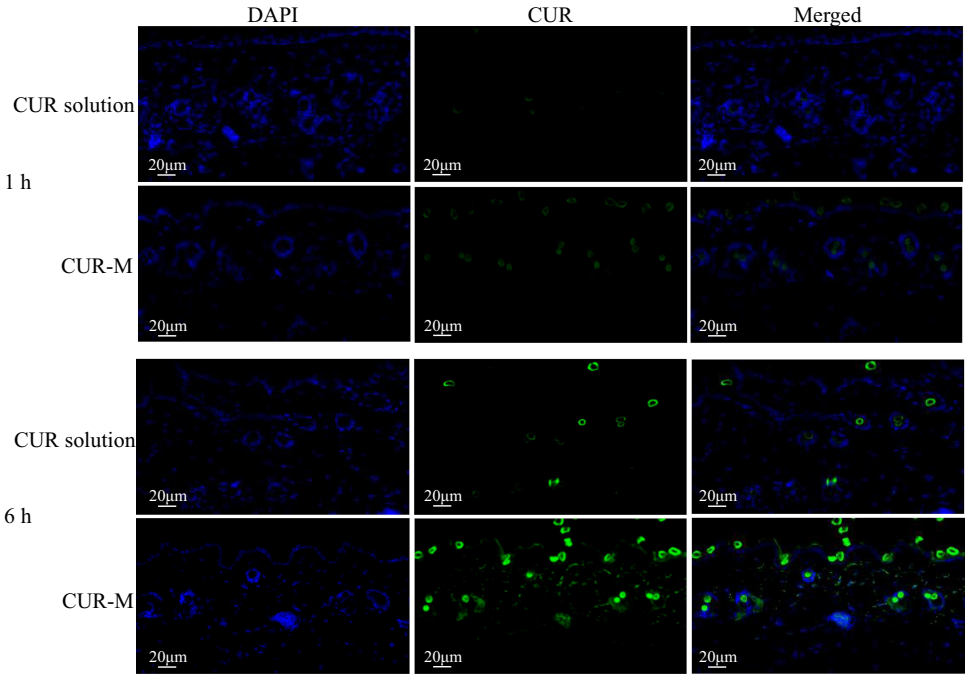

Figure 7 CLSM images of longitudinal section of the skins incubated with CUR solution and CUR-M at 1 h and 6 h.

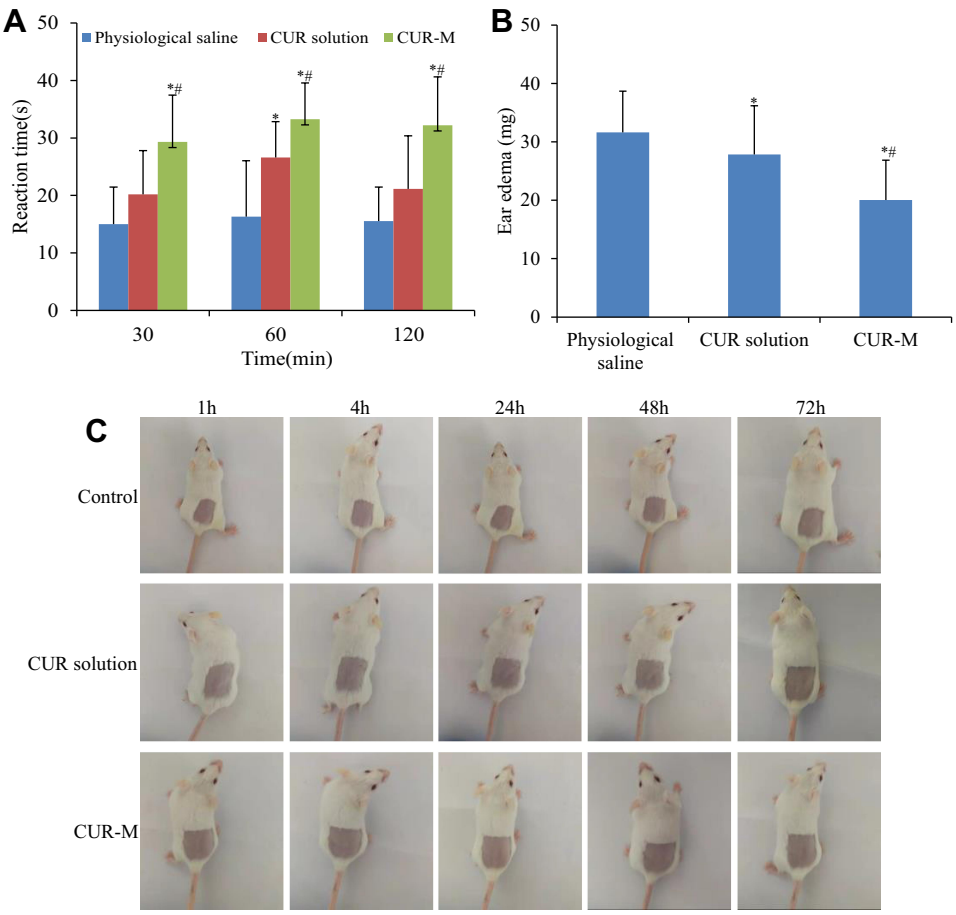

Figure 8 (**A**) Reaction time of physiological saline, CUR solution and CUR-M in mice at various time intervals (*p < 0.05 vs physiological saline group, #p < 0.05 vs CUR solution). (**B**) Effect of physiological saline, CUR solution and CUR-M on ear edema induced by dimethyl benzene in mice (*p < 0.05 vs physiological saline group, #p < 0.05 vs CUR solution). (**C**) In vivo skin irritation test. Skin appearance of mice observed at 1, 4, 24, 48 and 72 h after removing the residual formulation.

results of mean reaction time to thermal stimulation pain in mice at different time intervals after topical application of different formulations. According to Figure 8A, the transdermal administration of CUR-M (15 mg/kg) showed significantly prolonged reaction times of mice to thermal pain when compared with the physiological saline group and CUR solution group at all time points ($p<0.05$). The penetration and retention of CUR-M in mice skin were enhanced and resulted in higher skin bioavailability compared with CUR solution, which might be the main reason for the better analgesic effect of CUR-M. This result indicated that the developed CUR-M formulation was beneficial to improve the analgesic activity of the CUR.

Assessment of Anti-Inflammatory Activity

The topical anti-inflammatory activity of the formulation was evaluated using dimethyl benzene-induced ear edema in mice, ear edema and inhibitory ratios of ear edema were used as parameters to evaluate the anti-inflammatory effect of CUR-M. As can be seen from Figure 8B, the ear edema of CUR-M group was 20.03 ± 6.82 mg, while the ear edema of the CUR solution group was 27.85 ± 8.33 mg at the same dose, CUR-M significantly reduced ear edema compared with CUR solution ($p < 0.05$). The inhibitory ratios of ear edema of CUR solution and CUR-M were 8.02% and 34.20%, respectively. The developed formulation showed 4.26 times better effect than CUR solution. This result indicated that CUR-M showed better anti-inflammatory activity than CUR solution. The enhanced anti-inflammatory activity might be related to improvement of HA micelles for drug skin penetration and retention. The significant topical anti-inflammatory indicated that CUR-M might offer the additional advantage of relieving topical inflammatory disease. This established the usefulness of CUR-M as a better delivery system for topical effect of CUR-M.

In vivo Skin Irritation

The skin irritation of the formulations was investigated by visually observing whether the formulations could cause skin irritation or edema in mice. The results showed that the use of different formulations did not produce any skin irritation to the mice skin (Figure 8C). This result indicated that the CUR-M formulation had no skin irritation; therefore, it was safe for topical application, which would be beneficial for improving skin acceptability and patient compliance.

Conclusions

In this study, octadecylamine modified hyaluronic acid (OHA) copolymer was synthesized and used to formulate CUR-loaded micelles. The micelles formulated by HA effectively improved the stability and solubility of CUR and allowed the slow release of the loaded drug. It was obvious that micelle formulation was effective for the topical transdermal delivery of CUR. When compared to CUR solutions, the formulated CUR-loaded micelles exhibited higher skin penetration and deposition, better in vivo analgesic and anti-inflammatory activities and negligible skin irritation. In conclusion, the developed micelle formulation might have the potential for the treatment of topical pain and skin infections. Further evaluation is required to elucidate its clinical therapeutic effect.

Acknowledgments

We are grateful for the financial supports from the Key Scientific Research Project of Higher Education of Henan Province (No. 20B180006), the National project cultivation fund of Luoyang Normal University (No. 2019-PYJJ-012) and key scientific and technological project of Henan of China (No. 202102110103).

Disclosure

The authors report no conflicts of interest for this work.

References

1. Zhang Y, Xia Q, Li Y., et al. CD44 Assists the Topical Anti-Psoriatic Efficacy of Curcumin-Loaded Hyaluronan-Modified Ethosomes: a New Strategy for Clustering Drug in Inflammatory Skin. *Theranostics*. 2019;9(1):48–64. doi:10.7150/thno.29715
2. Kandekar SG, Singhal M, Sonaje KB, et al. Polymeric micelle nanocarriers for targeted epidermal delivery of the hedgehog pathway inhibitor vismodegib: formulation development and cutaneous biodistribution in human skin. *Expert Opin Drug Deliv*. 2019;16(6):667–674.
3. Ali MK, Moshikur RM, Wakabayashi R, et al. Biocompatible Ionic Liquid-Mediated Micelles for Enhanced Transdermal Delivery of Paclitaxel. *ACS Appl Mater Interfaces*. 2021;13(17):19745–19755.
4. Niu J, Yuan M, Chen C, et al. Berberine-Loaded Thiolated Pluronic F127 Polymeric Micelles for Improving Skin Permeation and Retention. *Int J Nanomedicine*. 2020;15:9987–10005.
5. Ahmed OAA, El-Say KM, Aljaeid BM, et al. Optimized vinpocetine-loaded vitamin E D-alpha-tocopherol polyethylene glycol 1000 succinate-alpha lipoic acid micelles as a potential transdermal drug delivery system: in vitro and ex vivo studies. *Int J Nanomedicine*. 2019;14:33–43.
6. Pensado A, McGrogan A, White KAJ, et al. Assessment of dermal bioavailability: predicting the input function for topical glucocorticoids using stratum corneum sampling. *Drug Deliv Transl Res*. 2022;12(4):851–861.
7. Desai P, Patlolla RR, Singh M. Interaction of nanoparticles and cell-penetrating peptides with skin for transdermal drug delivery. *Mol Membr Biol*. 2010;27(7):247–259.
8. Sintov AC, Levy HV, Greenberg I. Continuous Transdermal Delivery of L-DOPA Based on a Self-Assembling Nanomicellar System. *Pharm Res*. 2017;34(7):1459–1468.
9. Jiang K, Zhao D, Ye R, et al. Transdermal delivery of poly-hyaluronic acid-based spherical nucleic acids for chemogene therapy. *Nanoscale*. 2022;14(5):1834–1846.
10. Zhu J, Tang X, Jia Y, et al. Applications and delivery mechanisms of hyaluronic acid used for topical/transdermal delivery - A review. *Int J Pharm*. 2020;578:119127.
11. Anirudhan TS, Varghese S, Manjusha V. Hyaluronic acid coated Pluronic F127/Pluronic P123 mixed micelle for targeted delivery of Paclitaxel and Curcumin. *Int J Biol Macromol*. 2021;192:950–957.
12. Wan T, Pan W, Long Y, et al. Effects of nanoparticles with hydrotropic nicotinamide on tacrolimus: permeability through psoriatic skin and antipsoriatic and antiproliferative activities. *Int J Nanomedicine*. 2017;12:1485–1497.
13. Son SU, Lim JW, Kang T, et al. Hyaluronan-Based Nanohydrogels as Effective Carriers for Transdermal Delivery of Lipophilic Agents: towards Transdermal Drug Administration in Neurological Disorders. *Nanomaterials*. 2017;7(12):427.
14. Yuan M, Niu J, Xiao Q, et al. Hyaluronan-modified transfersomes based hydrogel for enhanced transdermal delivery of indomethacin. *Drug Deliv*. 2022;29(1):1232–1242.
15. Wichayapreechar P, Anuchapreeda S, Phongpradist R, et al. Dermal targeting of Centella asiatica extract using hyaluronic acid surface modified niosomes. *J Liposome Res*. 2020;30(2):197–207.

16. Sittisanguanphan N, Paradee N, Sirivat A. Hyaluronic Acid and Graphene Oxide-incorporated Hyaluronic Acid Hydrogels for Electrically Stimulated Release of Anticancer Tamoxifen Citrate. *J Pharm Sci*. 2022;111(6):1633–1641.
17. Zhu T, Yu X, Yi X, et al. Lidocaine-Loaded Hyaluronic Acid Adhesive Microneedle Patch for Oral Mucosal Topical Anesthesia. *Pharmaceutics*. 2022;14(4):686.
18. Slika L, Patra D. A short review on chemical properties, stability and nano-technological advances for curcumin delivery. *Expert Opin Drug Deliv*. 2020;17(1):61–75.
19. Abdel-Hafez SM, Hathout RM, Sammour OA. Curcumin-loaded ultradeformable nanovesicles as a potential delivery system for breast cancer therapy. *Colloids Surf B Biointerfaces*. 2018;167:63–72.
20. Zhang M, Asghar S, Jin X, et al. The enhancing effect of N-acetylcysteine modified hyaluronic acid-octadecylamine micelles on the oral absorption of paclitaxel. *Int J Biol Macromol*. 2019;138:636–647.
21. Song L, Pan Z, Zhang H, et al. Dually folate/CD44 receptor-targeted self-assembled hyaluronic acid nanoparticles for dual-drug delivery and combination cancer therapy. *J Mater Chem B*. 2017;5(33):6835–6846.
22. Zhong YN, Goltsche K, Cheng L, et al. Hyaluronic acid-shelled acid-activatable paclitaxel prodrug micelles effectively target and treat CD44-overexpressing human breast tumor xenografts in vivo. *Biomaterials*. 2016;84:250–261.
23. Abdallah MH, Abu Lila AS, Unissa R, et al. Preparation, characterization and evaluation of anti-inflammatory and anti-nociceptive effects of brucine-loaded nanoemulgel. *Colloids Surf B Biointerfaces*. 2021;205:111868.
24. Xavier-Santos JB, Felix-Silva J, Passos JGR, et al. Development of an effective and safe topical anti-inflammatory gel containing Jatropha gossypiifolia leaf extract: results from a pre-clinical trial in mice. *J Ethnopharmacol*. 2018;227:268–278.
25. Peters CA, Sgrott RAG, Peters RR, et al. Production of Wilbrandia ebracteata extract standardized in flavonoids and dihydrocurcubitacin and assessment of its topical anti-inflammatory activity. *Ind Crops Prod*. 2015;69:123–128.
26. Zhao YC, Zheng HL, Wang XR, et al. Enhanced Percutaneous Delivery of Methotrexate Using Micelles Prepared with Novel Cationic Amphipathic Material. *Int J Nanomedicine*. 2020;15:3539–3550.
27. Zhao Y, Zheng C, Zhang L, et al. Knockdown of STAT3 expression in SKOV3 cells by biodegradable siRNA-PLGA/CSO conjugate micelles. *Colloids Surf B Biointerfaces*. 2015;127:155–163.
28. Li JL, Shin GH, Lee IW, et al. Soluble starch formulated nanocomposite increases water solubility and stability of curcumin. *Food Hydrocoll*. 2016;56:41–49.
29. Tarrahi R, Khataee A, Karimi A, et al. Development of a cellulose-based scaffold for sustained delivery of curcumin. *Int J Biol Macromol*. 2021;183:132–144.
30. Nair RS, Morris A, Billa N, et al. An Evaluation of Curcumin-Encapsulated Chitosan Nanoparticles for Transdermal Delivery. *AAPS PharmSciTech*. 2019;20(2):69.
31. Nguyen TT, Neri TA, Choi BD. Characterization of hyaluronic acid extracted from Liparis tessellatus eggs grafted with phenolic acids and nisin. *Int J Biol Macromol*. 2020;157:45–50.
32. Duan Y, Zhang B, Chu L, et al. Evaluation in vitro and in vivo of curcumin-loaded mPEG-PLA/TPGS mixed micelles for oral administration. *Colloids Surf B Biointerfaces*. 2016;141:345–354.
33. McManamon C, Cameron A, de Silva JP, et al. Effect of cross-linking and hydration on microscale flat punch indentation contact to collagen-hyaluronic acid films in the viscoelastic limit. *Acta Biomaterialia*. 2020;111:279–289.
34. Zheng J, Shen CY, Pang JY, et al. [Preparation of tanshinone A loaded nanostructured lipid carrier and its in vitro transdermal permeation characteristics]. *Zhongguo Zhong Yao Za Zhi*. 2016;41(17):3232–3238. Chinese.
35. Faisal W, Soliman GM, Hamdan AM. Enhanced skin deposition and delivery of voriconazole using ethosomal preparations. *J Liposome Res*. 2018;28(1):14–21.
36. Witting M, Boreham A, Brodwolf R, et al. Interactions of hyaluronic Acid with the skin and implications for the dermal delivery of biomacromolecules. *Mol Pharm*. 2015;12(5):1391–1401.
37. Cilurzo F, Vistoli G, Gennari CG, et al. The role of the conformational profile of polysaccharides on skin penetration: the case of hyaluronan and its sulfates. *Chem Biodivers*. 2014;11(4):551–561.
38. Chen J, Ma YQ, Tao YY, et al. Formulation and evaluation of a topical liposomal gel containing a combination of zedoary turmeric oil and tretinoin for psoriasis activity. *J Liposome Res*. 2021;31(2):130–144.
39. Taweechat P, Pandey RB, Sompornpisut P. Conformation, flexibility and hydration of hyaluronic acid by molecular dynamics simulations. *Carbohydr Res*. 2020;493:108026.
40. Taieb M, Gay C, Sebban S, et al. Hyaluronic acid plus mannitol treatment for improved skin hydration and elasticity. *J Cosmet Dermatol*. 2012;11(2):87–92.
41. Lapteva M, Mondon K, Moller M, et al. Polymeric micelle nanocarriers for the cutaneous delivery of tacrolimus: a targeted approach for the treatment of psoriasis. *Mol Pharm*. 2014;11(9):2989–3001.
42. Jijie R, Barras A, Boukherroub R, et al. Nanomaterials for transdermal drug delivery: beyond the state of the art of liposomal structures. *J Mater Chem B*. 2017;5(44):8653–8675.
43. Kong J, Qiang W, Jiang J, et al. Safflower oil body nanoparticles deliver hFGF10 to hair follicles and reduce microinflammation to accelerate hair regeneration in androgenetic alopecia. *Int J Pharm*. 2022;616:121537.